Beta decay of ^{30}Na: Experiment and theory

P. Baumann, Ph. Dessagne, A. Huck, G. Klotz, A. Knipper, Ch. Miehé, M. Ramdane,* and G. Walter
Centre de Recherches Nucléaires et Université Louis Pasteur, 67037 Strasbourg, France

G. Marguier
Institut de Physique Nucléaire, 69622 Villeurbanne, France

H. Gabelmann, C. Richard-Serre, and K. Schlösser
ISOLDE Collaboration, European Organization for Nuclear Research (CERN), 1211 Geneva 23, Switzerland

A. Poves
Departamento de Fisica Teorica, C-XI, Universidad Autonoma, Cantoblanco, 28049 Madrid, Spain
(Received 1 November 1988)

The ^{30}Na β decay was studied on-line by means of mass-separation techniques. Gamma-ray, gamma-gamma, neutron-gamma spectra, neutron time-of-flight singles, and γ-coincidence measurements were registered. High-energy neutron branches ($E_n > 2$ MeV) were found complementing previously reported data. A ^{30}Na β-decay scheme to ^{30}Mg bound and unbound states is established. The distribution of the transition strength as a function of the excitation energy for particle-unbound levels in ^{30}Mg is compared to shell-model calculations performed in the 0–12 MeV excitation energy range. An overall renormalization yields a B(GT) quenching factor of 0.28 substantially lower than generally observed in this mass region. Three levels in ^{29}Mg which are strongly populated via the $1n$ channel are related to negative-parity intruder states.

I. INTRODUCTION

We have undertaken a study of the neutron- and gamma-emission modes which follow the beta decay of $^{29-31}$Na at the European Organization for Nuclear Research (CERN) on-line mass separator ISOLDE. A systematic analysis of the Gamow-Teller (GT) decay is in progress and a comparison is made with theoretical estimates in the *sd*-shell-model space.[1] For $A=29$, we found a remarkable agreement,[2] whereas for very neutron-rich sodium and magnesium isotopes around $A=31$, results[3–5] are rather in sharp contradiction with predictions based on the straightforward *sd*-shell model. The correct spin, $J^\pi = \frac{3}{2}^+$, is predicted for the ^{31}Na ground state by Watt *et al.*,[6,7] by taking into account the $1f_{\frac{7}{2}}$ orbit in the model space. Enlarging the Hilbert space more, Poves and Retamosa[8] additionally include the $2p_{\frac{3}{2}}$ orbit and reproduce consistently the experimental data by their calculations. This microscopic description concludes in favor of an onset of a rotational regime for $N=20$ and for $Z \geq 11$, corresponding to the nearly half-filled $1d_{\frac{5}{2}}$ orbit, and stimulates further measurements in this mass region.

It is noteworthy that the large Q_β values involved allow testing of the GT$^-$ operator for delayed neutron precursors. In the past, GT quenching studies could most often be carried out for mirror pairs, GT$^+$ decays or, more generally, for charge-transfer reactions.

The present work investigates the ^{30}Na beta decay by neutron and gamma spectroscopy. The hitherto unknown upper part of the GT strength B(GT) is deduced from the energy spectra of high-energy delayed neutrons observed for the first time. The time-of-flight technique and n-γ coincidence measurements were used. The low-

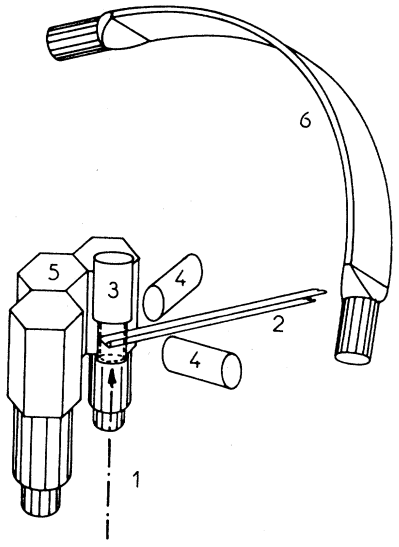

FIG. 1. Experimental setup. (1) ion beam, (2) tape, (3) $4\pi\beta$ detector, (4) γ counters, (5) NE213 cells, (6) curved scintillator.

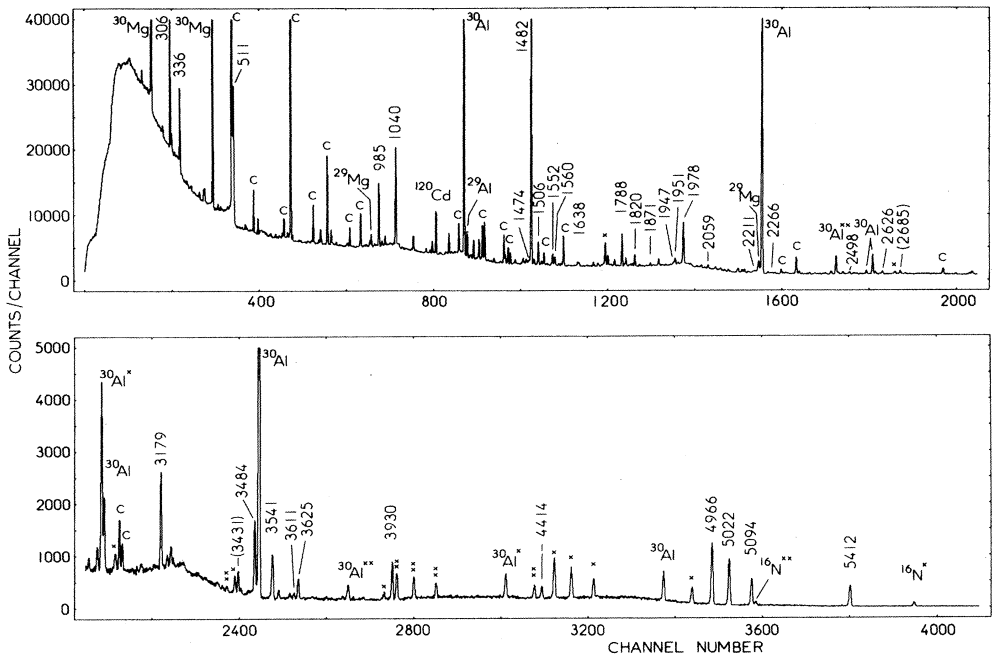

FIG. 2. Gamma-ray spectrum following β decay of ^{30}Na. The peaks attributed to the ^{30}Na decay are labeled with the corresponding γ-ray energy in keV; other lines are marked by the parent isotope. The comtaminant ^{120}Ag activity is labeled as *C*. Peaks marked with ($\times$) and ($\times\times$) correspond to single- and double-escape lines, respectively. The transitions with energies in parentheses observed in Ref. 5 remain unassigned.

energy ($E_n < 2$ MeV) spectrum of the delayed neutrons had been extensively studied by Ziegert *et al.*[9] by means of ^{3}He counters. The purpose of this investigation was to delimit the mass region where the nuclear properties can be understood in terms of *sd*-shell systematics and to locate possible intruder states by means of the beta-decay process.

II. EXPERIMENTAL PROCEDURE

The ^{30}Na nuclei were produced by bombarding a uranium carbide target with the 2μA proton beam of the 600 MeV CERN synchrocyclotron and afterwards ionized in a tungsten surface-ionization source. The yield achieved at the ISOLDE facility for ^{30}Na was typically 2×10^2

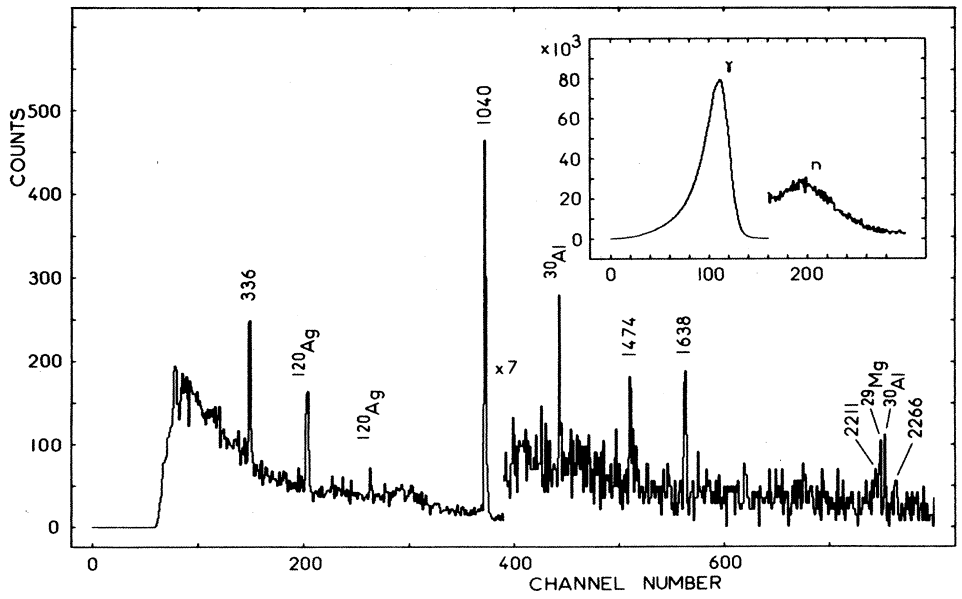

FIG. 3. Gamma spectrum in coincidence with the NE213 liquid scintillators. The inset shows the n-γ discrimination.

TABLE I. Energy and intensity of γ rays observed in the β decay of ^{30}Na. The 54.6 keV γ ray occurring in the ^{29}Mg deexcitation is not listed in the present table. The 4685 keV γ ray observed in Ref. 5 with a relative intensity of 2.2±1.0 is not seen in the present work with an upper limit of 0.3.

E_γ (keV)	I_γ (relative)	I_γ (per 100 decays)	Transition (MeV)
305.6±0.3	11.4±0.7	4.8±0.5	1.79–1.48
336.1±0.3[a]	6.3±0.4	2.7±0.3	1.43–1.09
985.1±0.4	14.5±0.9	6.2±0.7	2.47–1.48
1040.1±0.4[a]	25.3±1.5	10.8±1.1	1.09–0.05
1474.0±1.0[b]	0.69±0.15	0.29±0.06	1.47–0
1482.0±0.3	100	42.3±3.1	1.48–0
1505.8±0.4	8.4±0.6	3.6±0.5	4.97–3.46
1552.4±0.4	4.7±0.4	2.0±0.3	5.09–3.54
1559.6±0.4	3.6±0.3	1.5±0.2	5.02–3.46
1638.0±0.6[a]	1.9±0.3	0.8±0.1	1.64–0
1788.0±0.7	4.0±0.6	1.7±0.4	1.79–0
1820.2±0.6	5.4±0.4	2.3±0.3	1.82–0
1870.7±1.0	1.3±0.2	0.6±0.1	5.41–3.54
1947.0±0.8	1.6±0.3	0.7±0.1	4.41–2.47
1951.5±0.7	4.5±0.3	2.0±0.2	5.41–3.46
1978.0±0.6	24.7±1.5	10.5±1.1	3.46–1.48
2059.0±0.6	2.0±0.3	0.8±0.1	3.54–1.48
2211.0±1.0[a]	1.2±0.3	0.5±0.1	2.27–0.05
2266.0±1.0[a]	0.3±0.1	0.13±0.05	2.27–0
2497.8±1.3	1.8±0.2	0.8±0.1	4.97–2.47
2626.0±1.3	2.3±0.3	1.0±0.1	5.09–2.47
3178.8±1.0	12.6±0.9	5.4±0.7	4.97–1.79
3484.0±1.0	12.1±0.8	5.1±0.5	4.97–1.48
3541.1±1.1[c]	6.7±0.7	2.8±0.5	3.54–0
3541.1±1.1	1.6±0.7	0.7±0.5	5.02–1.48
3611.0±1.4	0.8±0.1	0.3±0.1	5.09–1.48
3625.0±1.1	3.1±0.3	1.3±0.2	5.41–1.79
3929.7±1.3	6.6±0.5	2.8±0.3	5.41–1.48
4414.4±1.5	2.5±0.2	1.1±0.2	4.41–0
4966.5±1.2	16.2±1.0	6.9±0.7	4.97–0
5021.7±1.2	12.7±0.8	5.4±0.6	5.02–0
5094.3±1.2	7.4±0.5	3.1±0.4	5.09–0
5411.8±1.2	6.4±0.4	2.7±0.3	5.41–0

[a]Subsequent to one-neutron emission.
[b]Subsequent to two-neutron emission.
[c]Doublet.

atoms/s in this experiment. The experimental setup for observing the decay of this short-lived isotope ($T_{1/2}$=50±3 ms, Ref. 5) was arranged around the collection point located on the mylar ribbon of a tape transport system as shown in Fig. 1. In this way, the descendant and contaminant activities could be reduced by driving the tape with a constant velocity of 30 cm/s. The collection point was surrounded by a thin cylindrical β detector which delivered the triggering signal attesting a beta decay and was used in particular as a start in the neutron time-of-flight measurement. A large area (2880 cm^2) plastic scintillator sheet (thickness: 1.25 cm) bent in a curvature radius of 100 cm, was used with a time resolution of 1.1 ns for neutron spectroscopy. The counter was operated with a recoil proton detection threshold typically set at 1.0 MeV. In order to compare our data with the low-

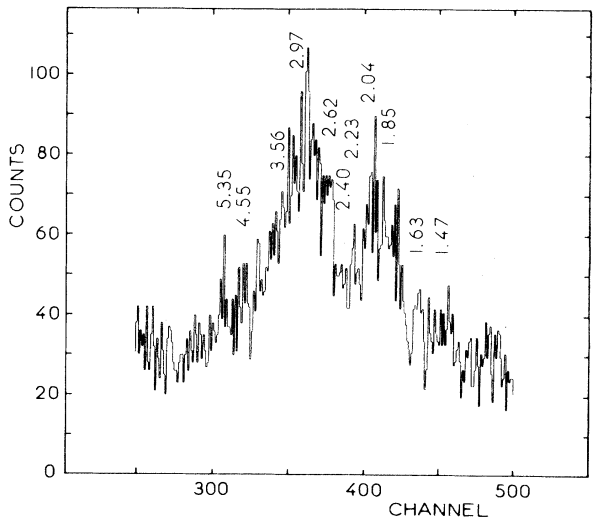

FIG. 4. Neutron time-of-flight spectrum related to the ^{30}Na decay.

energy spectrum of Ziegert *et al.* and to observe n-γ coincidences at low neutron energy, a separate measurement was performed with a threshold set at the minimum (0.4 MeV) at the cost of time resolution and background level. A description of the experimental arrangement is given elsewhere.[10] Two Ge(Li) counters were used to per-

TABLE II. Gamma-ray branching ratios in ^{30}Mg.

E_i (keV)	E_f (keV)	Gamma branching ratios
1482	0	100
1788	0	26±3
	1482	74±3
1820	0	100
2467	1482	100
3460	1482	100
3541	0	80±12
	1482	20±12
4414	0	61±7
	2467	39±7
4966	0	32±2
	1482	24±1
	1788	24±1
	2467	4±1
	3460	16±1
5021	0	71±6
	1482	9±6
	3460	20±3
5094	0	49±2
	1482	5±1
	2467	15±2
	3541	31±2
5412	0	29±2
	1482	30±2
	1788	14±1
	3460	21±1
	3541	6±1

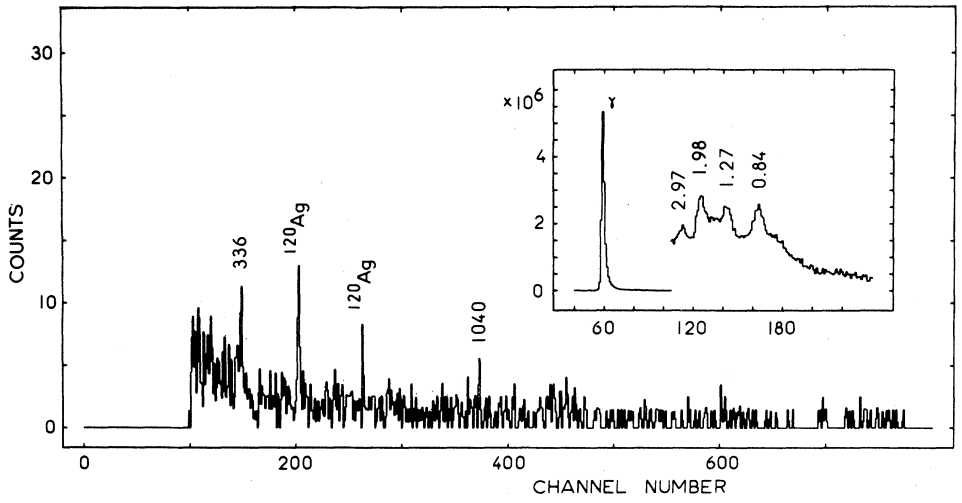

FIG. 5. Gamma spectrum in coincidence with the curved spectrometer with a gate on neutron energies in the 1.5 MeV region. In the inset, the time-of-flight spectrum registered with the low threshold (see text) is represented.

form γ-ray singles, γ-γ, and n-γ coincidence measurements. The detection efficiency of the n-γ coincidences was ensured by a neutron filter consisting in three hexagonal cells (active volume per cell: 3750 cm^3) filled with NE213 scintillator. In order to identify unambiguously the gamma-ray emitters, the n-γ coincidences were registered in a biparametric mode (E_γ vs n-γ discrimination signal) which allows a check that a gamma line subsequent to a neutron event did not result from γ-γ coincidences due to an insufficient rejection in the pulse-shape discrimination.

III. EXPERIMENTAL RESULTS

The gamma-ray spectrum observed in the ^{30}Na decay is shown in Fig. 2. The identified peaks belong to the decay of the $A=30$ chain or to the decay of the contaminant ^{120}Ag nucleus produced with the same settings of the beam line, because of charge and mass numbers ($4+$, $A=120$) proportional to the corresponding values for the sodium ions ($1+$, $A=30$).

TABLE III. Beta intensities and logft values in the ^{30}Na β decay to bound levels in ^{30}Mg.

E_x (keV)	I_β (per 100 decays)	logft[a]
1482.0±0.3	11.2±2.6	5.8
1787.8±0.4	<0.6	>7.0
1820.2±0.6	2.3±0.3	6.4
2467.1±0.5	3.7±0.5	6.1
3460.0±0.7	3.5±0.7	6.0
3541.1±1.1	1.2±0.4	6.5
4414.4±1.2	1.7±0.2	6.2
4966.2±0.5	21.8±1.7	5.0
5021.3±2.2	7.6±0.6	5.5
5093.7±0.7	6.5±0.6	5.5
5412.2±0.6	9.3±0.8	5.3

[a]The error on the logft values is typically of the order of ±0.1 and is calculated with $Q_\beta=17.30\pm0.24$ MeV, $T_{1/2}=50$ ms, and $P_\gamma=68.85\%$.

The energy and intensity of 33 gamma rays in the ^{30}Na decay have been measured and are listed in Table I along with the corresponding assignments in ^{30}Mg. The occurrence of a doublet is stated at 3541 keV, of which the components are alloted to definite transitions with the help of coincidence data. Gamma-ray branching ratios in ^{30}Mg are reported in Table II. Several discrepancies with previous results[5] react unavoidably on the β branching and logft values. In particular, the 336 keV transition which is assigned by Guillemaud *et al.*[5] to the $A=30$ chain is found to belong to the ^{29}Mg decay scheme. As usual in this type of decay scheme work, a number of weak, unassigned lines are left over. Excitation energies, β intensities and the corresponding logft values for bound levels in ^{30}Mg populated in the decay of ^{30}Na are listed in Table III. The intensities of the β branches are deduced from the imbalances of the gamma intensities connected with each level. Values given in Refs. 4 and 5 for $T_{1/2}$, Q_β, P_n, and in Ref. 11 for log$f$ have been used for the log$f$ computing.

For ^{30}Na, $1n$-, $2n$-, and alpha-delayed emissions have been reported previously with $P_{1n}=30\pm4$, $P_{2n}=1.15\pm0.25$ (Ref. 5), and $P_\alpha=(5.5\pm2)\times10^{-5}$ (Ref. 12) per 100 β decays. The interest of our measurement with time-of-flight techniques was to search for high-energy neutron emissions together with relevant information on n-γ coincidences and so to complement previous results[9] related to low-energy delayed neutrons.

The gamma spectrum taken in coincidence with the neutron filter (Fig. 3) reveals lines at 336, 1040, 1638, 2211, and 2266 keV. On the basis of our results on ^{29}Na β decay (Ref. 2) and the present n-γ coincidence data, it is inferred that five excited states (55, 1095, 1431, 1638, and 2266 keV) of ^{29}Mg are populated after β-delayed one-neutron emission in the ^{30}Na decay. The 1431 keV level is identified with the 1.46±0.04 MeV state observed

by Fifield *et al.*[13] in the ^{26}Mg(^{18}O,^{15}O)^{29}Mg reaction. The existence of the 2266 keV level is directly linked to the observation of the 2211–2266 keV γ doublet, the energy difference of which corresponds to the ^{29}Mg ground-state doublet spacing. Branching ratios for transitions from the 2266 keV level to the $\frac{3}{2}^+$ and $\frac{1}{2}^+$ components are, respectively, 20±5 and 80±5. Experimentally, a level was observed at 2.20±0.04 MeV in the 3n-transfer reaction,[13] at 2.34±0.09 MeV in the ^{26}Mg(^{11}B,^{8}B)^{29}Mg reaction[14] and at 2.21±0.09 MeV in the ^{13}C(^{18}O,2p)^{29}Mg reaction.[15]

In the two-neutron channel, the population of the 1474 keV excited level in ^{28}Mg is disclosed by the n-γ coincidences (Fig. 3), the deexciting γ line is enhanced, besides, by the higher detection probability of the corresponding 2n event. Nearby 30% of the 2n emission involves this 2^+ level. To our knowledge this is the first evidence for the population of an excited state in a 2n channel. We are presumably in a situation where all favoring conditions are joined together for the observation of a possible dineutron process[16] corresponding to a $l=0$, $\Delta J=0$ transition from a 2^+ level in ^{30}Mg. These

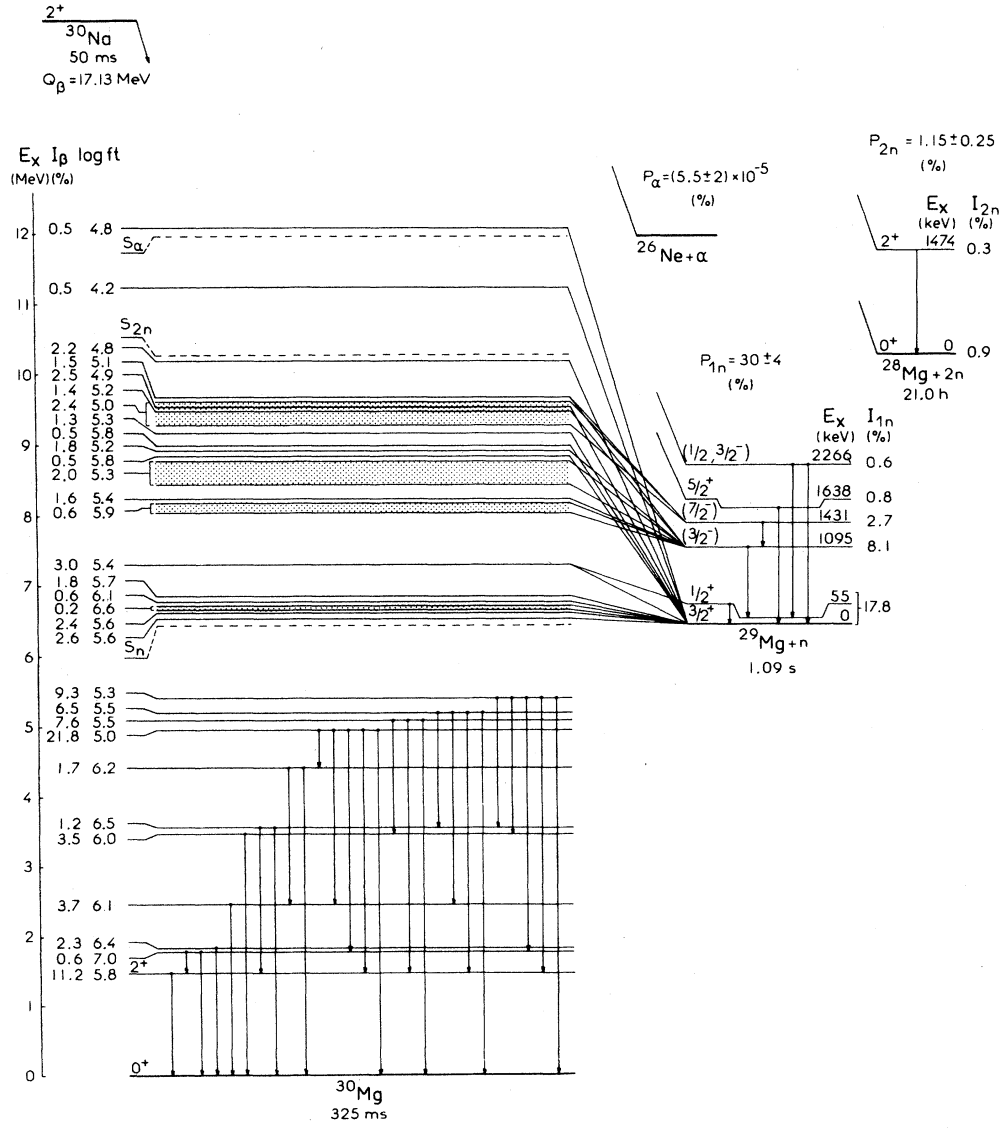

FIG. 6. ^{30}Na β-decay scheme showing excitation energies and γ transitions deduced from γ and neutron spectroscopy. For the low-energy part of the particle-unbound states we make use of the data obtained by Ziegert *et al.* (Ref. 9). P_n, P_{2n}, and P_α values are taken from Refs. 5 and 12. The shaded areas correspond to unresolved neutron groups in the time-of-flight spectrum. In so far as ^{30}Na has a ground-state spin and parity 2^+ (Ref. 5), the logft values calculated in this work assign an angular momentum 1, 2, 3 and a positive parity to all states placed in this decay scheme above 4.9 MeV except the levels weakly fed in the 6.5–6.7 MeV region.

TABLE IV. Beta branching, logft values of unbound levels in ^{30}Mg inferred from the measured spectrum of delayed-neutron emissions from ^{30}Mg.

E_n[a] (MeV)	E_γ coinc. (^{29}Mg)[b] (keV)	E_x (^{30}Mg)[c] (keV)	I_β (per 100 decays)	logft
0.071		6515	2.6±0.4	5.6
0.115		6561	2.4±0.4	5.6
(0.145–0.220)		(6592–6672)	0.2±0.1	6.6
0.242		6692	0.6±0.1	6.1
0.375		6830	1.8±0.3	5.7
(0.500–0.635)	1040	(8054–8194)	0.6±0.1	5.9
0.668	1040	8228	1.6±0.2	5.4
0.795	55	7319	3.0±0.5	5.4
0.847		7319		
(0.900–1.200)	1040	(8468–8778)	2.0±0.3	5.3
1.267	1040	8848	1.8±0.3	5.2
(1.380–1.680)	336	(9300–9611)	2.4±0.3	5.0
1.87±0.06	1040	9470±220	1.4±0.2	5.2
2.07±0.08	1040	9677±230	1.5±0.2	5.1
2.27±0.09		8792±250	0.5±0.1	5.8
2.44±0.10		8962±270	0.5±0.1	5.8
2.66±0.12		9192±295	1.3±0.2	5.3
3.02±0.14		9562±325	2.5±0.4	4.9
3.62±0.20		10182±380	2.2±0.3	4.8
4.63±0.30		11230±485	0.5±0.1	5.2
5.464±0.40		12090±600	0.5±0.1	4.8

[a]Values lower than 1680 keV are taken from Ref. 9. Unfortunately, no relevant error is known. The other values are from this work. Indications between parentheses refer to energy regions in the neutron spectra from which no prominent peak emerges and are likely related to unresolved neutron branches. This does not necessarily mean that the emitting level is broad.

[b]Neutron branches nonevidently connected to a coincident γ ray from the final nucleus are considered to feed the ground state in ^{29}Mg as the P_{2n} value is markedly lower than the P_{1n} one.

[c]These energies are deduced from considerations sketched out in footnote a taking into account the recoil energy of the final nucleus, and a neutron separation energy in ^{30}Mg equal to 6440±210 keV (Ref. 17).

results stimulate further studies in this field. The neutron spectrum, measured with the curved scintillator is represented in Fig. 4. The relative intensities of the different components, after detector response correction, are reported in Table IV taking into account the efficiency and a detection threshold at 1 MeV which results in a decrease of the intrinsic efficiency from 9.8% at 1.7 MeV to 8.5% around 6 MeV. Evidence for n-γ coincidences has been found for different neutron groups (Table IV) in the low-threshold experiment. As an example we report in Fig. 5 the γ spectrum registered in coincidence with a 1.38–1.68 MeV neutron gate on the time-of-flight spectrum. Two γ lines (336 keV, 1040 keV) are clearly observed, the 336 keV one appearing only with this particular gate.

TABLE V. Neutron branching in the one- and two-neutron emissions by ^{30}Mg subsequent to β decay of ^{30}Na and deduced from γ-intensity analysis. The P_{1n}(30±4) and P_{2n}(1.25±0.25) values are taken from Ref. 5.

E_x (^{29}Mg) (keV)	I_{1n} (per 100 decays)	E_x (^{28}Mg) (keV)	I_{2n} (per 100 decays)
0			
55	17.8±4.0	0	0.9±0.3
1095	8.1±1.1	1474	0.3±0.1
1431	2.7±0.3		
1638	0.8±0.1		
2266	0.6±0.1		

Normalization between the results of Ziegert *et al.*[9] and ours has been carried out using the intensity of the 1.68–2.28 MeV region measured in both experiments. The β branching ratios to the neutron-emitting states are obtained by normalizing the total intensity of the neutron lines to the known 1n-emission probability (P_{1n}=30%, Ref. 5) and are listed in Table IV along with the corresponding logft values. Table V gives the absolute intensity of the various neutron branches to ^{28}Mg and ^{29}Mg levels obtained from γ imbalances. One should notice the very weak attained values owing to the acuteness of the γ-spectroscopy techniques. The established ^{30}Na β-decay scheme to particle-bound and particle-unbound states in ^{30}Mg is presented in Fig. 6.

The dominant feature of the measured delayed-neutron emission is the evidence of several strong branches deexciting high-lying levels in ^{30}Mg and corresponding to an important fraction of the Gamow-Teller strength in the ^{30}Na decay. The high-energy part of the delayed-neutron spectrum is interpreted by the decay of levels up to 12 MeV in ^{30}Mg, markedly above the 2n-separation energy

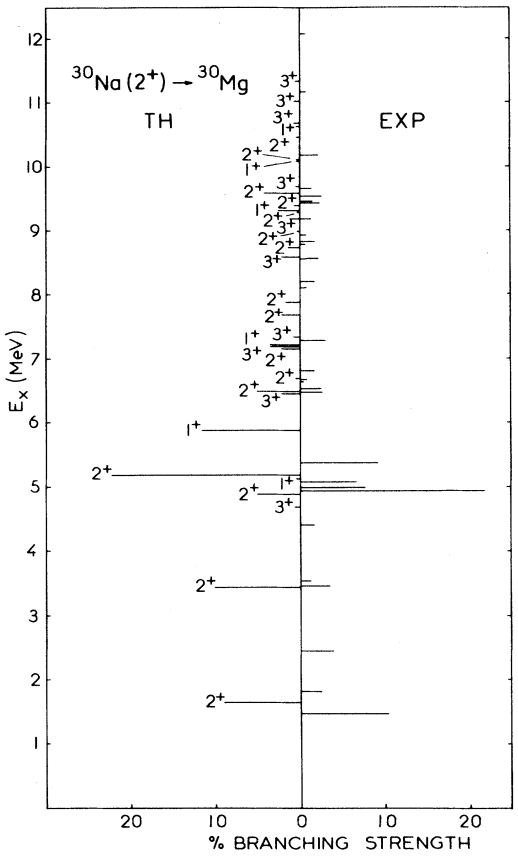

FIG. 7. Experimental and theoretical values (Ref. 1 and this work) for beta branching strength in the beta decay of ^{30}Na.

($S_{2n}=10.23\pm0.23$ MeV, Ref. 17). Due to the weakness of the $2n$ process, the corresponding emitting levels in ^{30}Mg could not be located.

The most frequency neutron process is the $1n$ emission. In order to test the validity of the decay scheme corresponding to this channel, it is interesting to check the absolute strength of the 1040 keV γ ray deexciting the second level in ^{29}Mg which is representative of the almost whole neutron strength towards ^{29}Mg except the ground-state doublet. This quantity can be determined in two independent ways: (i) the summation of all neutron branch intensities observed in coincidence with this line; (ii) from its absolute intensity as measured in the direct γ spectrum. The first calculation yields 11.3 ± 0.7 per 100 β decays in excellent agreement with 10.8 ± 1.1 deduced from the second one. This result shows that the present decay scheme gives an exhaustive description of the neutron branching to excited states above 55 keV in ^{29}Mg, if one takes for granted the P_n value.

IV. DISCUSSION

The new results obtained for the β decay of ^{30}Na in the $0n$ and $1n$ channels can be compared to calculations using the complete *sd*-model space[1] or including configurations with two neutrons promoted to the $1f\frac{7}{2}$ and $2p\frac{3}{2}$ orbits.[8] The spin of the ground state of ^{30}Na is $J=2$ (Ref. 5) and a positive parity is expected from systematics and theoretical predictions. Therefore, the experimental study of allowed beta decay yields significant information on positive parity states in ^{30}Mg in the spin range $j=1-3$. An important enlightenment is furthermore obtained for negative-parity states in ^{29}Mg, populated via the $1n$ channel.

A. Positive-parity states in ^{30}Mg

The ^{30}Na nucleus is a transitional one—in the sense of transition to deformation—and may have $2p$-$2h$ mixing in the ground state. Nevertheless, a previous work[8] has indicated that the $(sd)^{-2}(fp)^2$ configurations are small in the ground-state wave function of both ^{30}Na and ^{30}Mg and therefore a meaningful comparison between our results and calculations with a model space limited to *sd* shells is not irrelevant.

The excitation energies in the GT beta decay of ^{30}Na and the corresponding branching ratios have been given

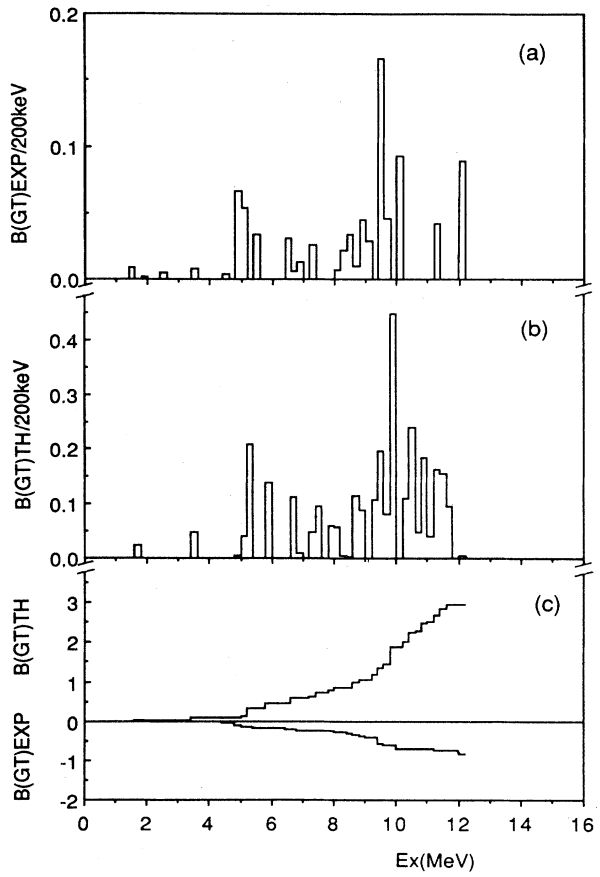

FIG. 8. B(GT) strength distribution for the beta decay of ^{30}Na. (a) Experimental and (b) theoretical strengths within each 200 keV energy interval are summed up and plotted as histograms. Note the change in the vertical scale between (a) and (b). (c) Integral of the GT strengths.

in Ref. 1 for the 24 lowest positive-parity states with $J^{\pi}=1^{+}$, 2^{+}, or 3^{+} spin values. The detection of the delayed-neutron emission allows a measurement of the strength for most of the energetically accessible states. Therefore, we have expanded the *sd* calculation in order to include daughter levels up to 12 MeV. The predicted Gamow-Teller strengths have been obtained using the free-nucleon operator.

In Fig. 7, we have reported experimental values for the beta branching strength and the corresponding theoretical values. In this comparison, we take notice of all the transitions observed without distinction between weak allowed decays and possible first forbidden ones. It appears that the two most intense measured transitions (to the 1482 and 4966 keV levels) are correctly reproduced by the calculation whereas the strong branch predicted towards the second 2^{+} model state ($E_x=3446$ keV) is not observed. In the experiment, two levels are found around the predicted energy (3460 and 3541 keV) with, for the second one, a γ branching ratio consistent with $J^{\pi}=2^{+}$ but a very weak β feeding ($1.2\pm0.4\,\%$).

A comparison between predicted and measured values is presented in Fig. 8 where we have reported differential and integral representations of B(GT). The differential plot of B(GT) vs excitation energy reveals a maximum of strength near 10 MeV excitation energy. Notice the good agreement between the shapes of the experimental and theoretical GT-distribution functions. However, the comparison of the intensities shows that the total experimental GT strength represents only 28% of the theoretical expectation under 12 MeV. The total half-life calculated in the *sd*-model space ($T_{1/2}=17.7$ ms) is shorter than the experimental value ($T_{1/2}=50\pm3$ ms).

Nevertheless, the inclusion of two particle-two-hole components in the theoretical calculation can reduce the discrepancy between theory and experiment. If the amount of *sd* components in ^{30}Na and ^{30}Mg is α^2 and β^2, respectively, the norm quenching due to the intruder mixing is $\alpha^2\beta^2$ and the remaining quenching factor $0.28/\alpha^2\beta^2$. The values of α^2 and β^2 are not well determined in the present state of the calculations, but, reasonable amounts of 2p-2h mixing could raise the quenching factor up to ≈ 0.4.

Finally, it is important to recall that a complete com-

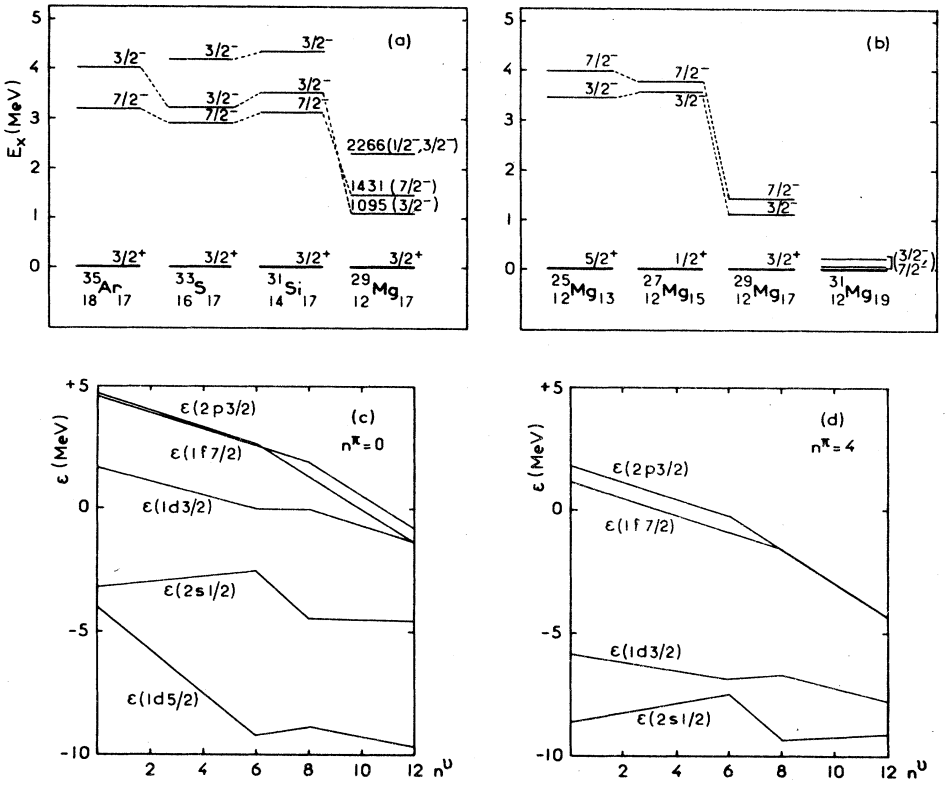

FIG. 9. In the upper part the lowest negative-parity states are presented for: (a) The $N=17$ isotones. (b) The odd-mass $^{25-31}$Mg isotopes. Results are taken from Ref. 22 and this work. The location at very low excitation energy of the $\pi(-)$ states in ^{31}Mg is deduced from a first detailed comparison between experiment (Refs. 5 and 19) and shell-model predictions in the ^{31}Na decay. In the lower part the effective energies of single-particle (s.p.) levels are presented as a function of the number of neutrons (n^{ν}) in the *sd* orbits. (c) The calculated variation for oxygen isotopes ($n^{\pi}=0$). (d) The calculated variation for magnesium isotopes ($n^{\pi}=4$).

parison between experiment and theory should involve the detection of the pairs of neutrons emitted in the $2n$ channel which was not possible with the present setup.

B. Negative-parity states in ^{30}Mg

From the values reported in Table III for the β branching ratios, the possibility of populating negative-parity states in ^{30}Mg through first forbidden transitions cannot be ruled out. No experimental evidence has been found in the γ-decay properties of ^{30}Mg levels, allowing to resolve the ambiguity in the parity of ^{30}Mg levels. Calculations in the lines of Ref. 8 predict negative-parity levels starting at 4 MeV excitation energy.

C. Negative-parity states in ^{29}Mg

Three levels located below $E_x=3$ MeV in ^{29}Mg cannot be related to the *sd*-model states ($E_x=1095$, 1431, and 2266 keV). They have no measurable beta feeding in the ^{29}Na decay but are strongly populated in the $1n$ channel of ^{30}Na. A $J^\pi=\frac{7}{2}^-$ value is proposed for the 1431 keV level which presents a single gamma branch ($E_\gamma=336$ keV) to the $J^\pi=\frac{3}{2}^-$ level at 1095 keV. The 1431 keV state previously observed in the (^{18}O,^{15}O) study[13] was tentatively assigned to a $(s\frac{1}{2})^2 f\frac{7}{2}$ configuration. The $\frac{3}{2}^-$ state resulting from the $(s\frac{1}{2})^2 p\frac{3}{2}$ configuration would then correspond to the 1095 keV level. These assignments are supported by the recent results of Woods *et al.*[18] obtained in the study of the ^{30}Si(^{13}C,^{14}O)^{29}Mg reaction. In this experiment, a strong population of the 1095 and 1431 keV levels was observed and found similar to the populations of the $\frac{3}{2}^-$ ($E_x=3.56$ MeV) and $\frac{7}{2}^-$ ($E_x=3.76$ MeV) levels in ^{27}Mg via the ^{28}Si(^{13}C,^{14}O)^{27}Mg reaction. For the 2266 keV level, $J^\pi=\frac{1}{2}^-$, $\frac{3}{2}^-$ is proposed, the negative-parity is favored by the neutron transmission coefficient (see below). We note that the $N=17$ isotones, ^{31}Si and ^{33}S, have a second $\frac{3}{2}^-$ state roughly located 1 MeV above the lowest one.

If we consider the systematics of the $N=17$ isotones [Fig. 9(a)], it appears for $Z=12$ as a sharp decrease in the excitation energy of the lowest negative-parity states, particularly for the $\frac{3}{2}^-$ level which comes below the $\frac{7}{2}^-$ one. The lowering of the $\frac{7}{2}^-$ orbit by the large neutron excess has been discussed by Storm *et al.*[7] We have reported in Fig. 9(b) the systematics of the lowest negative-parity states of the odd-mass $^{25-31}$Mg isotopes which show the drop of the excitation energy for $N\geq 17$. Previous results[5] on ^{31}Mg have revealed three states under 250 keV ($E_x=0$, 50, and 220 keV) which are confirmed by our work.[19] Shell-model calculations with *sd* or $(sd)^{-2}(fp)^2$ configurations can account for only one state in this excitation energy range. Thus we conclude that two of these states are good candidates for the lowest negative-parity states in ^{31}Mg. We have reported the effective energy of single-particle levels as a function of the number n^ν of *sd*-shell neutrons for the isotopes of oxygen [Fig. 9(c)] and magnesium [Fig. 9(d)]. The "USD" (unified *sd*) interaction of Wildenthal[20] is used for the *sd*-shell matrix elements whereas the *fp* and *sd*-*fp* matrix elements are taken from the calculation of Kahana *et al.*[21] with the modifications of Ref. 8. The most significant feature is the similar sharp decrease of the $2p\frac{3}{2}$ and $1f\frac{7}{2}$ excitation energy with increasing neutron number in agreement with experimental results.

The selectivity of the delayed-neutron emission leading to negative-parity states is very apparent in the ^{30}Na decay and clearly illustrated by the n-γ spectrum reported in Fig. 3. This selectivity is expected from the transmission coefficient T_l calculated with the optical model for different l values. In this mass region $l=1$ waves are strongly favored and can account for the selective population of the $(\frac{3}{2},\frac{7}{2})^-$ states in ^{29}Mg from the $(1,2,3)^+$ GT parent states in ^{30}Mg.

V. SUMMARY AND CONCLUSIONS

In this work, we have investigated the beta decay of ^{30}Na, taking into account a large range of available β-ray energies. The distribution of the experimental GT strength is found in fair agreement with the predictions made in a *sd*-shell-model space but the overall reduction with regard to the free-nucleon GT transition is more important than the one observed for nuclei in the upper part of the *sd* shell. The mixing due to the intruder states, precursors of the onset of deformation at $A=32$, can be partly responsible for this unusually large quenching. The present study has supplied spectroscopic information on odd-parity states in ^{29}Mg illustrating the importance of $1f\frac{7}{2}$ and $2p\frac{3}{2}$ shells substantially below the region of strong deformation. Finally, we are aware that a proper account of the GT decay in ^{30}Na necessitates the inclusion of the $2n$-decay channel which will be a next step in the β-decay analysis of neutron-rich nuclei far from stability.

*Present address: Université des Sciences et de la Technologie Houari Boumédiène, Institut de Physique, B.P. 32, El Alia, Alger, Algérie.

[1]B. H. Wildenthal, M. S. Curtin, and B. A. Brown, Phys. Rev. C **28**, 1343 (1983).

[2]P. Baumann, Ph. Dessagne, A. Huck, G. Klotz, A. Knipper, G. Marguier, Ch. Miehé, M. Ramdane, C. Richard-Serre, G. Walter, and B. H. Wildenthal, Phys. Rev. C **36**, 765 (1987).

[3]C. Thibault, R. Klapisch, C. Rigaud, A. M. Poskanzer, R. Prieels, L. Lessard, and W. Reisdorf, Phys. Rev. C **12**, 644 (1975).

[4]C. Detraz, M. Langevin, M. C. Goffri-Kouassi, D. Guillemaud, M. Epherre, G. Audi, C. Thibault, and F. Touchard, Nucl. Phys. **A394**, 378 (1983).

[5]D. Guillemaud-Mueller, C. Detraz, M. Langevin, F. Naulin, M. de Saint Simon, C. Thibault, F. Touchard, and M. Epherre, Nucl. Phys. **A426**, 37 (1984).

[6]A. Watt, R. P. Singhal, M. H. Strom, and R. R. Whitehead, J. Phys. G **7**, L145 (1981).

[7]M. H. Storm, A. Watt, and R. R. Whitehead, J. Phys. G **9**, L165 (1983).

[8]A. Poves and J. Retamosa, Phys. Lett. B **184**, 311 (1987).

[9]W. Ziegert, L. C. Carraz, P. G. Hansen, B. Jonson, K. L. Kratz, G. Nyman, H. Ohm, H. L. Ravn, and A. Schröder, Proceedings of the 4th International Conference on Nuclei Far from Stability, Helsingör, 1981, European Organization for Nuclear Research Report CERN 81-09, 1981, p. 327.

[10]A. Huck, G. Klotz, A. Knipper, Ch. Miehé C. Richard-Serre, G. Walter, A. Poves, H. L. Ravn, and G. Marguier, Phys. Rev. C **31**, 2226 (1985).

[11]Ph. Dessagne and Ch. Miehé, Centre de Recherches Nucléaires Internal Report PN 87-08, 1987.

[12]C. Detraz, M. Langevin, D. Guillemaud-Mueller, A. C. Mueller, C. Thibault, F. Touchard, G. Klotz, Ch. Miehé, G. Walter, M. Epherre, and C. Richard-Serre, Nucl. Phys. **A402**, 301 (1983).

[13]L. K. Fifield, P. V. Drumm, M. A. C. Hotchkis, T. R. Ophel, and C. L. Woods, Nucl. Phys. **A437**, 141 (1985).

[14]D. K. Scott, B. G. Harvey, D. L. Hendrie, L. Kraus, C. F. Maguire, J. Mahoney, Y. Terrien, and K. Yagi, Phys. Rev. Lett. **33**, 1343 (1974).

[15]A. D. Panagiotou, P. K. Kakanis, E. M. Gazis, M. Bernas, C. Detraz, M. Langevin, D. Guillemaud, and E. Plagnol, Z. Phys. A **302**, 117 (1981).

[16]V. I. Goldansky, Nucl. Phys. **19**, 482 (1960).

[17]A. H. Wapstra and G. Audi, Nucl. Phys. **A432**, 55 (1985).

[18]C. L. Woods, W. N. Catford, L. K. Fifield, N. A. Orr, and R. J. Sadleir Nucl. Phys. **A476**, 392 (1988).

[19]P. Baumann, Ph. Dessagne, A. Huck, G. Klotz, A. Knipper, G. Marguier, Ch. Miehé, M. Ramdane, C. Richard-Serre, G. Walter, and A. Poves (unpublished).

[20]B. H. Wildenthal, Prog. Part. Nucl. Phys. **11**, 5 (1983).

[21]S. Kahana, H. C. Lee, and K. Scott, Phys. Rev. **180**, 956 (1969).

[22]P. M. Endt and C. van der Leun, Nucl. Phys. **A310**, 1 (1978).